Electronic Supplementary Material (ESI) for Journal of Materials Chemistry A.

Microcrystalline Cellulose-derived Porous Carbons with Defective Sites for Electrochemical Applications

Hao Lu,† Linzhou Zhuang,† Rohit Ranganathan Gaddam, Xiaoming Sun, Changlong Xiao, Timothy Duignan, Zhonghua Zhu and X. S. Zhao*

School of Chemical Engineering, The University of Queensland, St Lucia, Brisbane, QLD 4072, Australia.

*Correspondence to george.zhao@uq.edu.au.

† These authors contributed equally to this work

SC working electrode preparation process and performance calculation equations

For SCs, the working electrodes were prepared by mixing 75 wt% active materials, 20 wt% CB conductive additive and 5 wt% polytetrafluoro ethylene binder. Then the mixture was pressed onto a stainless-steel mesh or nickel foam and dried at 60 °C for 24 h.

The specific gravimetric capacitance of a single electrode measured in a three-electrode system, C_m (in F/g), was obtained according to the following equation

$$C_m = I \vartriangle t/mV \quad (1)$$

C_m value derived from GCD in a two-electrode analysis was calculated from equation

$$C_m = 4I \vartriangle t/2mV \quad (2)$$

The specific areal capacitance C_s (in mF/cm^2) derived from GCD in a two-electrode analysis was calculated from equation

$$C_s = 4I \triangle t/2SV \tag{3}$$

The energy and power density, *E (Wh/Kg)* and *P (kW/Kg)*, of a SC cell were calculated from equations

$$E = 0.5C\,V^2/4 \times 3.6 \tag{4}$$

$$P = 3.6E\,/\triangle t \tag{5}$$

where, *i* is the instantaneous current response, *V* is the potential window, *Δt* is the discharge time, *m* is the mass and *S* is the geographic area of active materials on a single electrode.

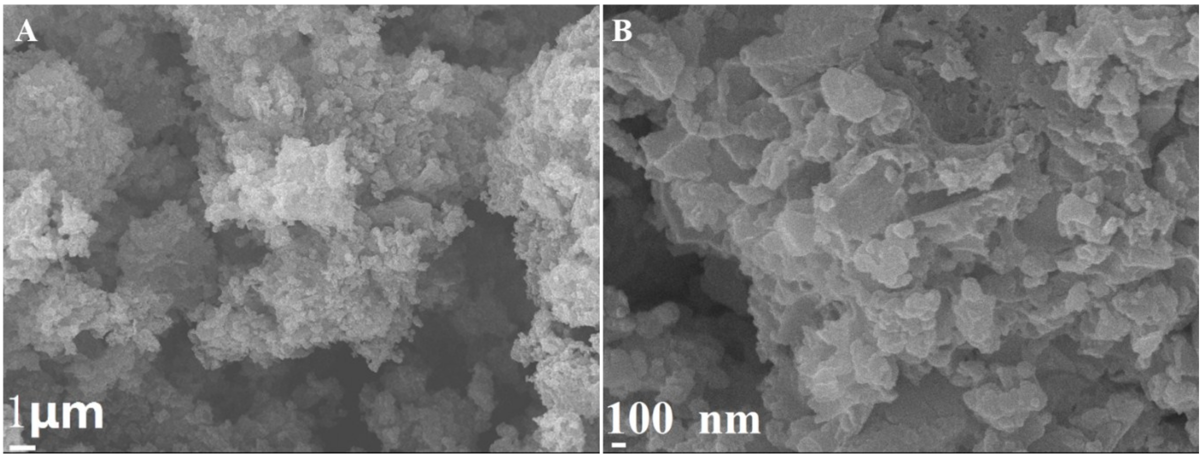

Fig. S1: FE-SEM images of the sample CNUY-600.

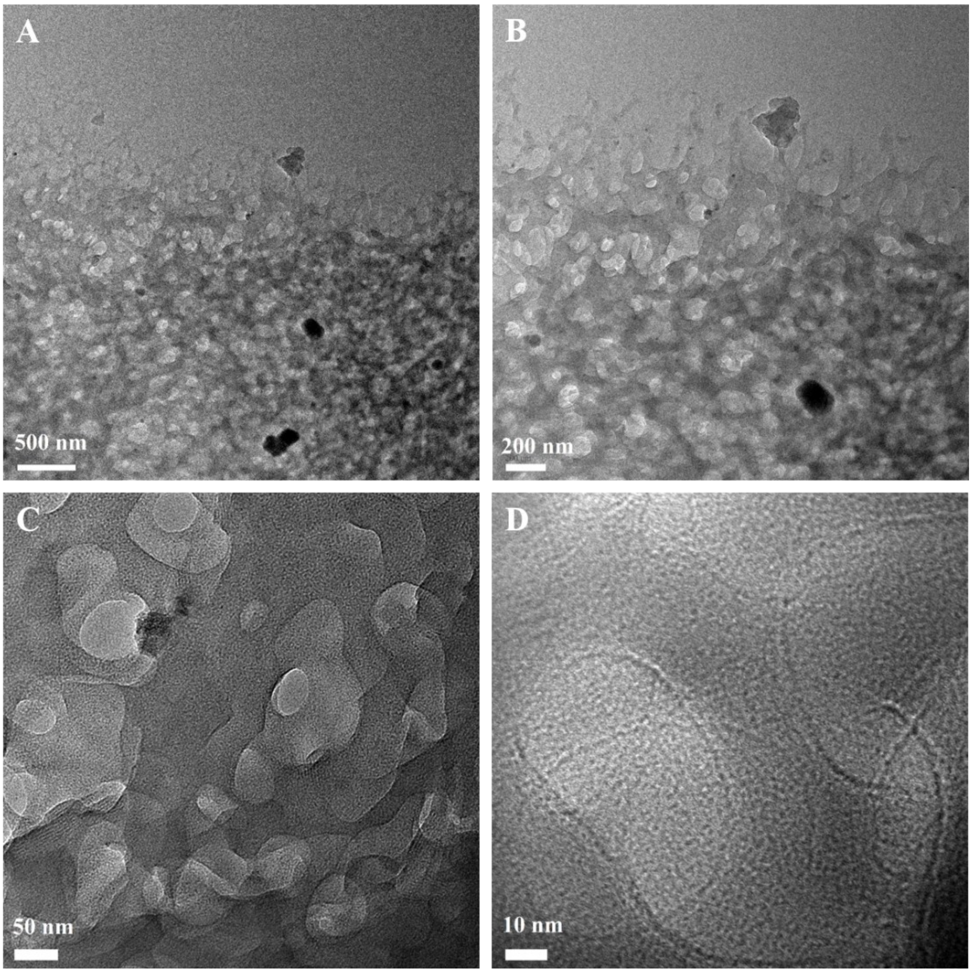

Fig. S2: TEM images of the sample CNUY-600.

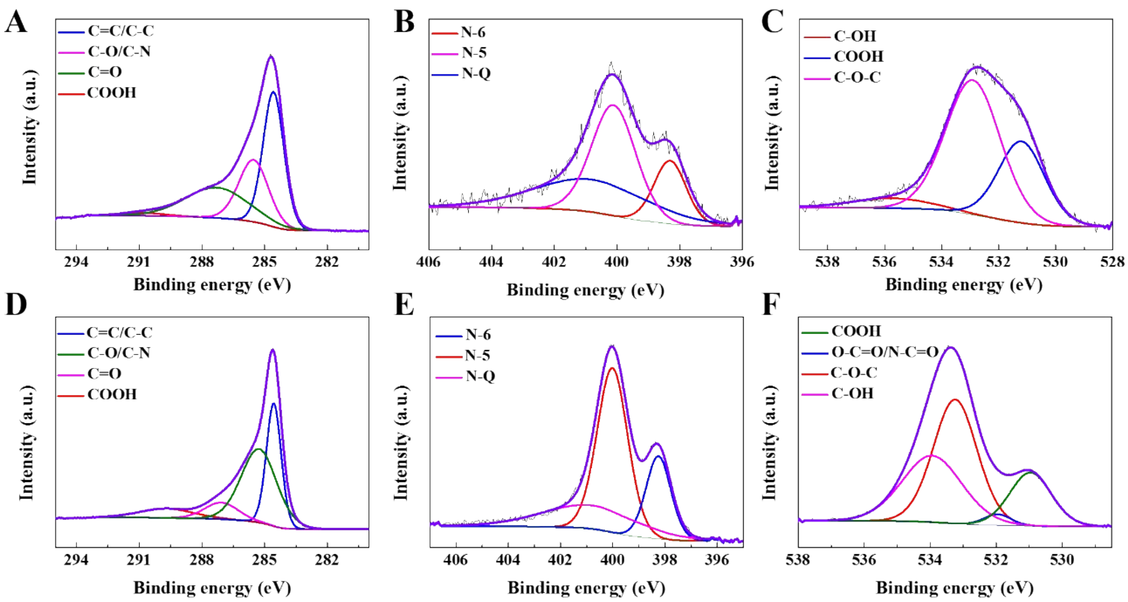

Fig. S3 The deconvoluted C 1s (A), N 1s (B), O 1s (C) spectra of sample CNUY-600H; The deconvoluted C 1s (D), N 1s (E), O 1s (F) spectra of CNUY-600.

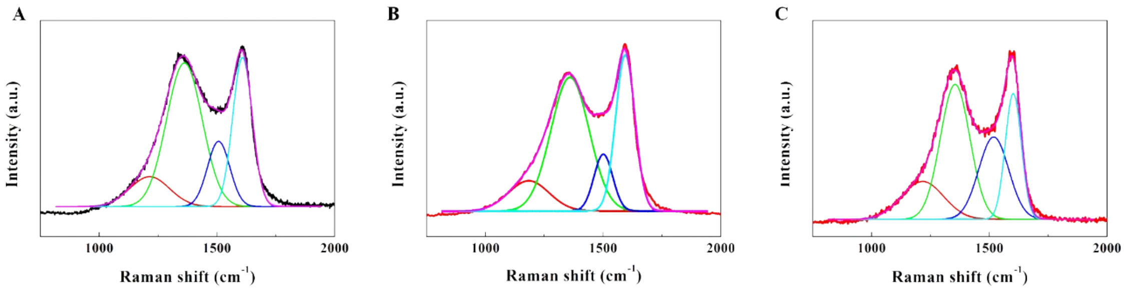

Fig. S4. Raman spectra of CNUY-600 (A), CNUY-600H (B) and CNUY-1100 (C) through Gaussian fitting. The I_G/I_D ratio of them is 1.03, 1.17 and 0.93, respectively.

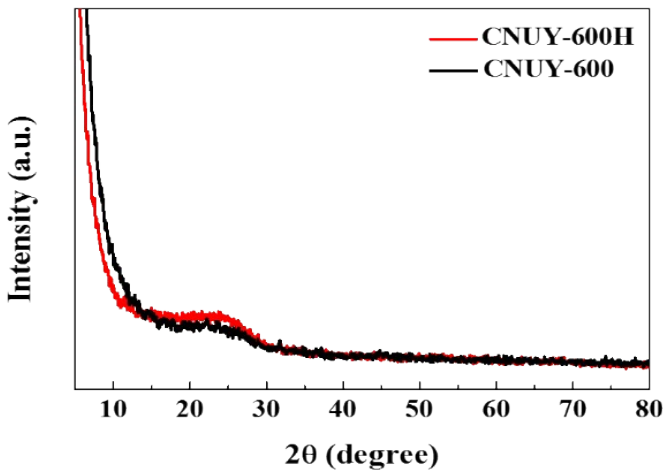

Fig. S5. XRD patterns of CNUY-600 and CNUY-600H.

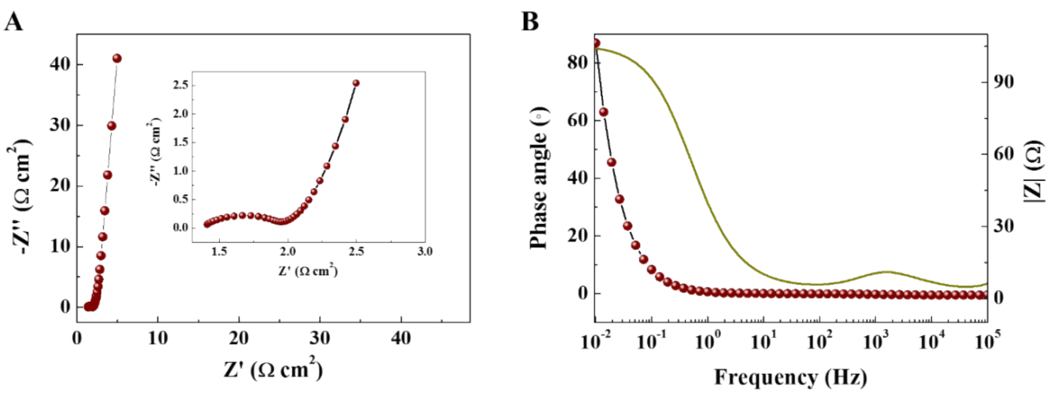

Fig. S6: The Nyquist plot (A) and Bode plots (B) of CNUY-600H measured in a three-electrode system with 1 M H_2SO_4 as the aqueous electrolyte.

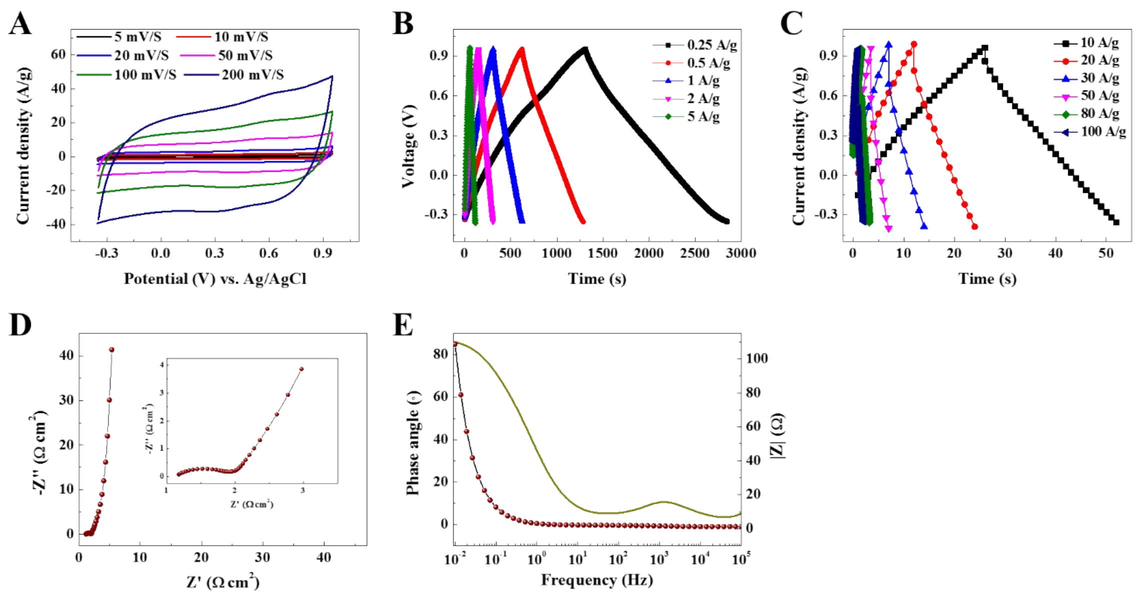

Fig. S7: The electrochemical performance of electrode CNUY-600 measured in a three-electrode system with 1 M H_2SO_4 as the aqueous electrolyte: CV curves at scan rates ranging from 5 mV/s to 200 mV/s (A), GCD curves at current densities from 0.25 to 100 A/g (B, C), Nyquist plot (D) and Bode plots (E).

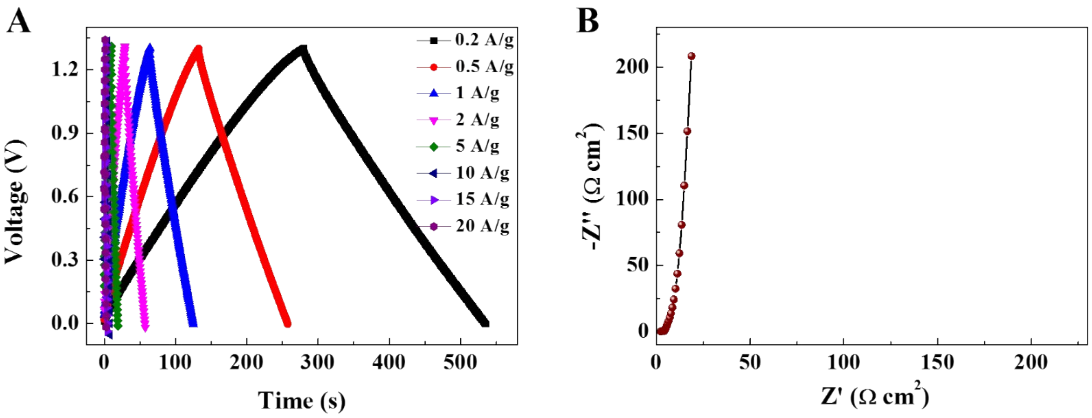

Fig. S8: The electrochemical performance of electrode CNUY-600 measured in a symmetric cell with 1 M H_2SO_4 aqueous electrolyte: GCD curves at different current densities (A), Nyquist plot (B).

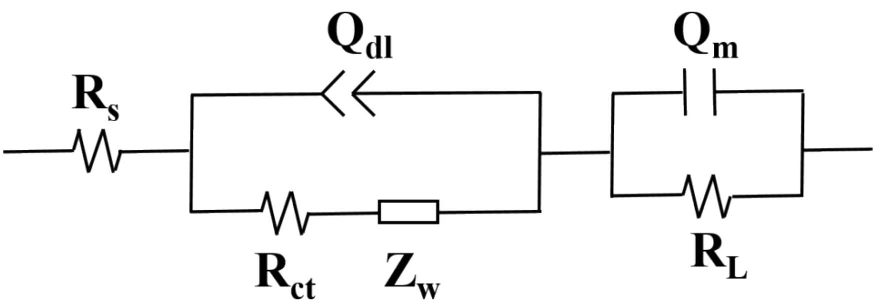

Fig. S9: The equivalent circuit used for fitting the Nyquist and Bode plots.

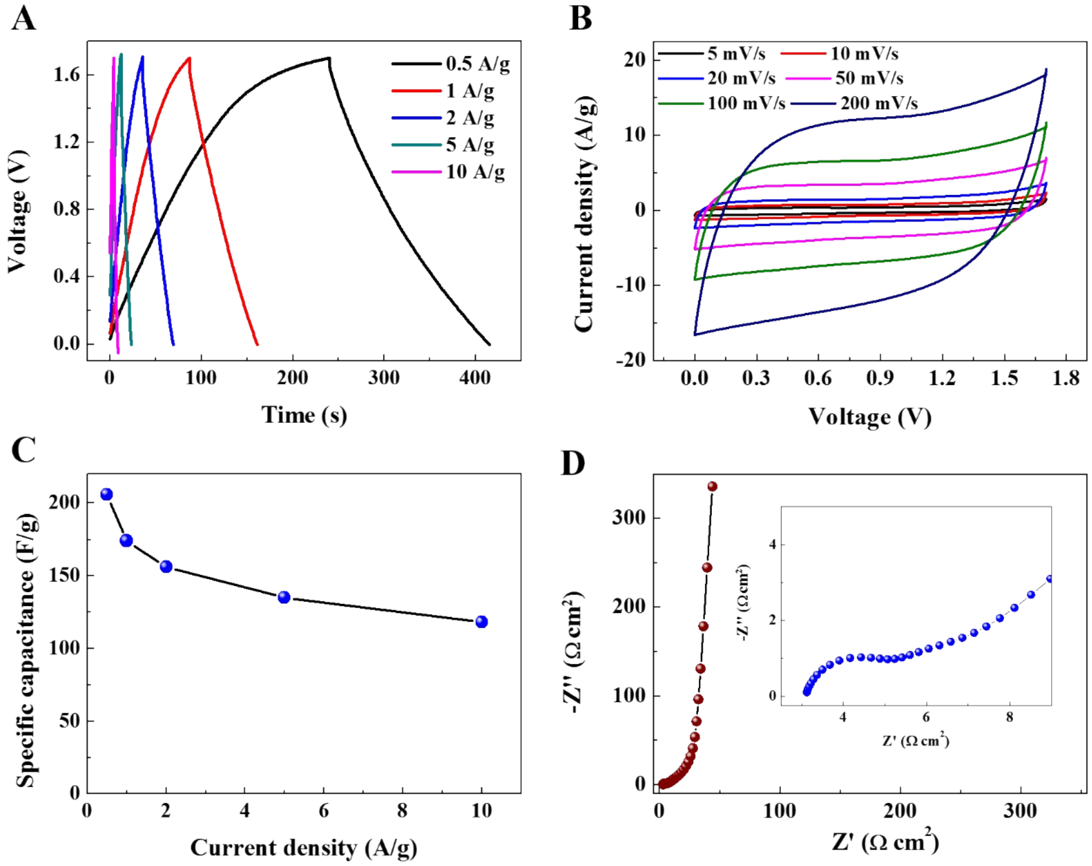

Fig. S10: The electrochemical performance of the electrode CNUY-600H measured in a symmetric cell with 1 M LiCl as the aqueous electrolyte: GCD curves at current densities ranging from 0.2 to 10 A/g (A), CV curves at scan rates from 5 to 200 mV/s (B), rate capability plot (C), Nyquist plot (D).

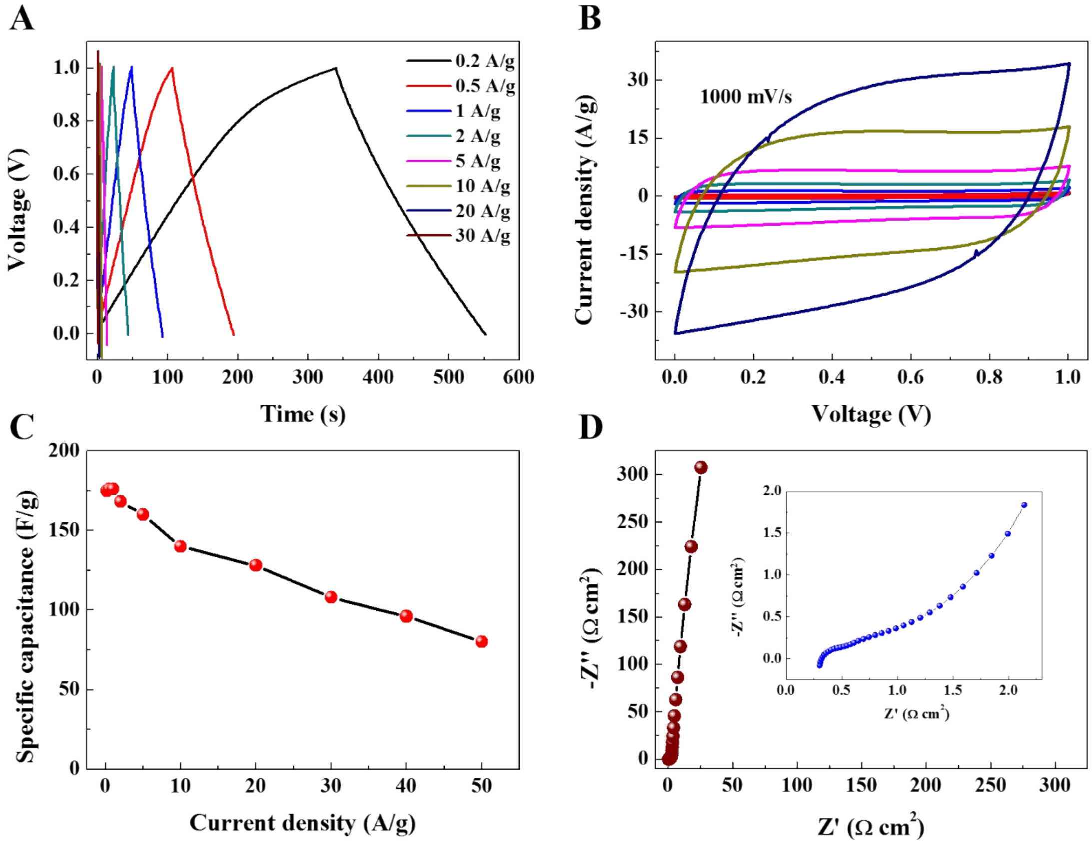

Fig. S11: The electrochemical performance of electrode CNUY-600H measured in a symmetric cell with 2 M KOH aqueous electrolyte: GCD curves at current densities ranging from 0.2 to 30 A/g (A), CV curves at scan rates from 5 to 1000 mV/s (B), rate capability plot (C), Nyquist plot (D).

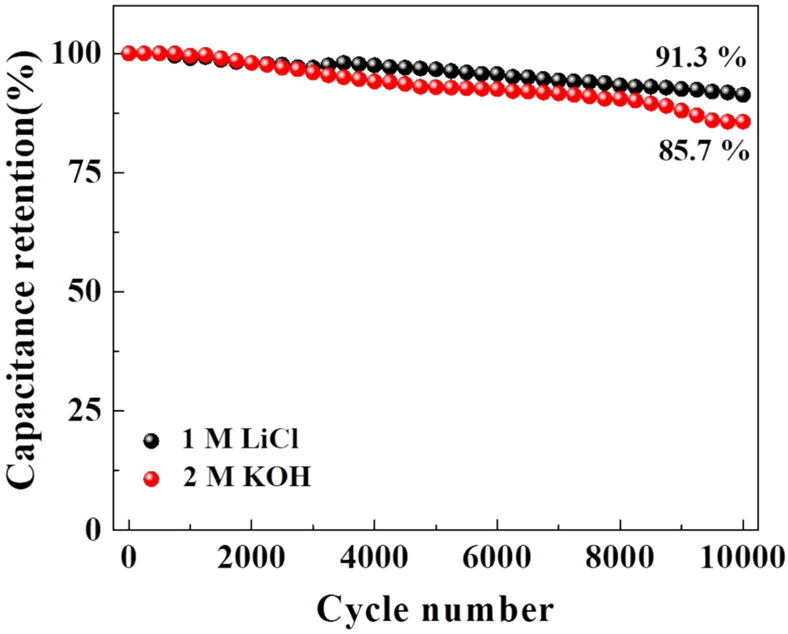

Fig. S12: Cycling performance of electrode CNUY-600H measured in a symmetric supercapacitor cell at a current density of 5A/g within 1 M LiCl and 2M KOH aqueous electrolyte.

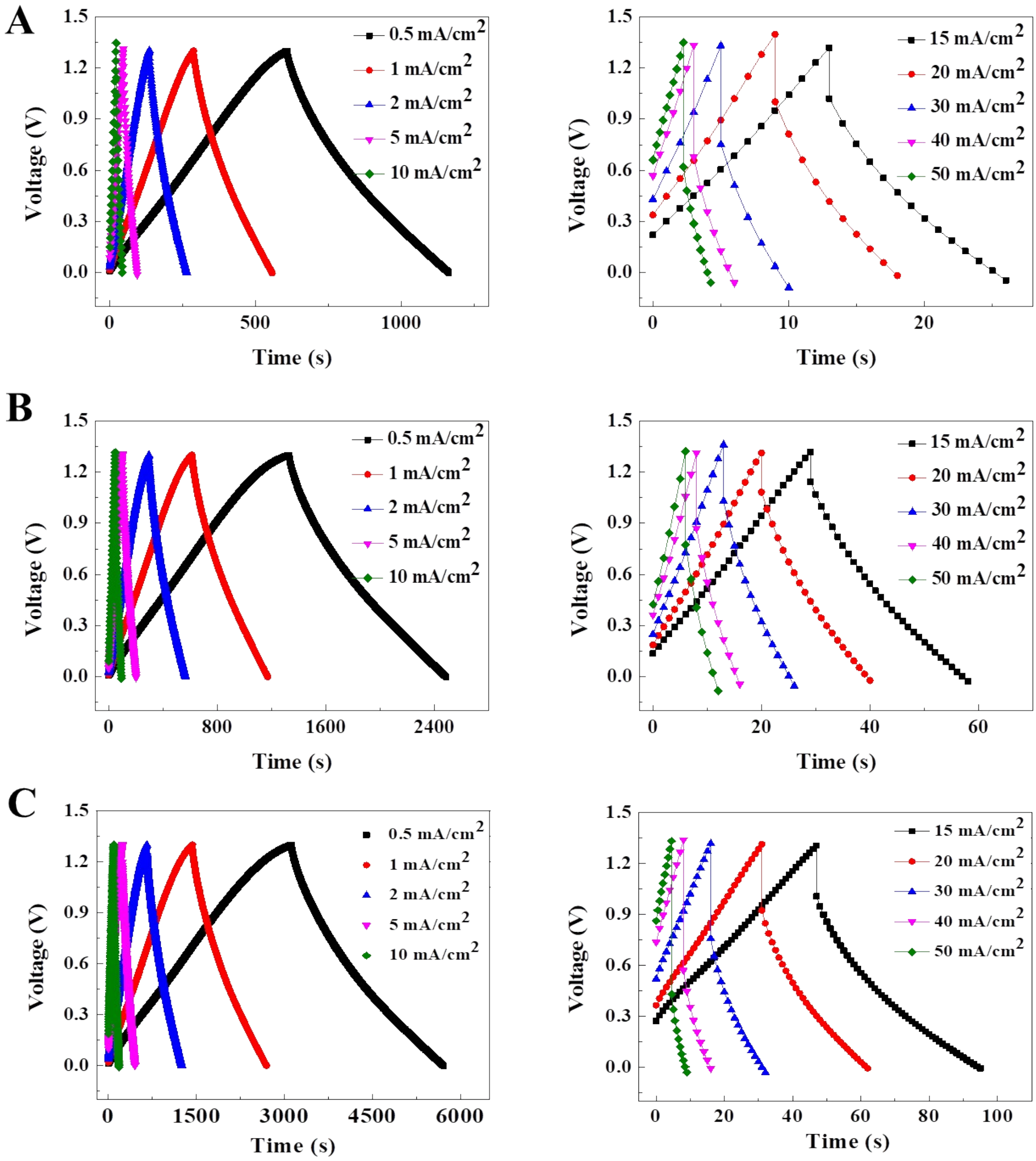

Fig. S13: GCD curves of electrode CNUY-600H with a mass loading of 4 mg/cm^2 (A), 8 mg/cm^2 (B) and 20 mg/cm^2 (C) at different current densities measured in a symmetric supercapacitor cell within 1 M H_2SO_4 aqueous electrolyte.

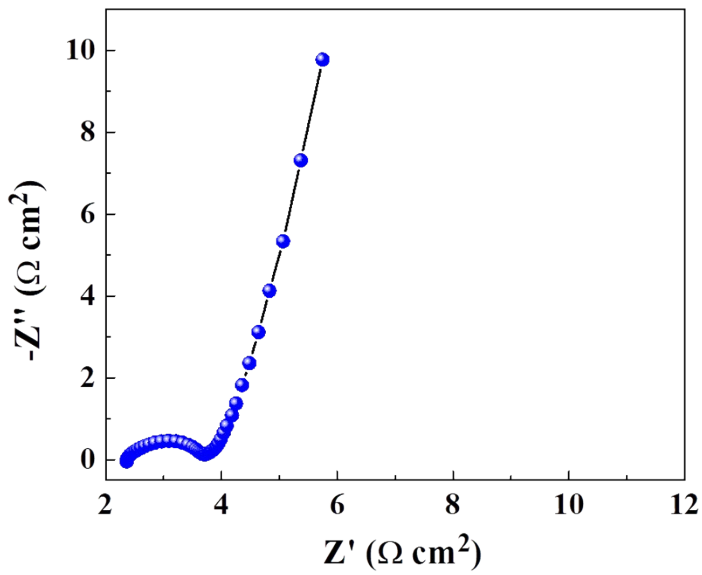

Fig. S14: Nyquist plot of electrode CNUY-600H with a mass loading of 20 mg/cm^2 measured in a symmetric cell within 1 M H_2SO_4 aqueous electrolyte.

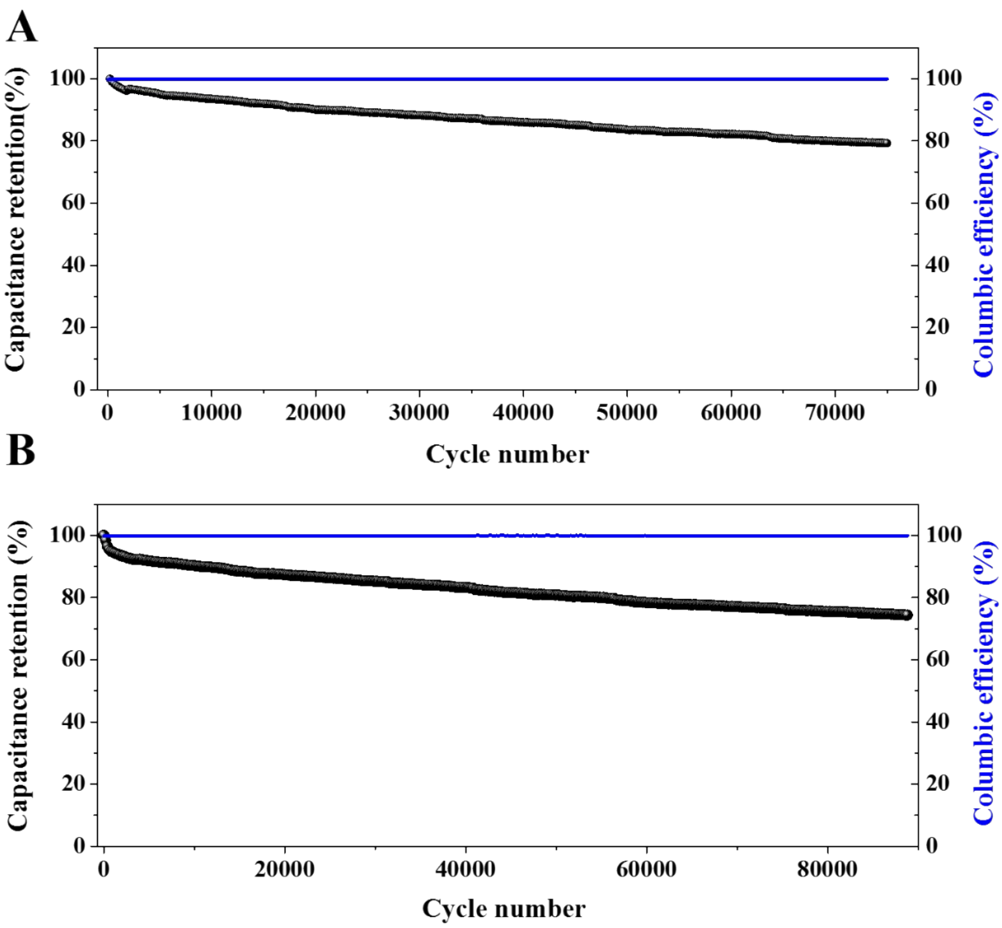

Fig. S15: Cycling performance of electrode CNUY-600H with a mass loading of 8 mg/cm^2 (A) and 12 mg/cm^2 (B) measured in a symmetric supercapacitor cell within 1 M H_2SO_4 aqueous electrolyte.

8 mg/cm^2: ~78 % of the initial areal capacitance value was maintained after 90000 cycles at a current density of 30 mA/cm^2

12 mg/cm^2: ~81 % and ~75% of the initial areal capacitance value was maintained after 50000 and 90000 cycles at a current density of 30 mA/cm^2 respectively.

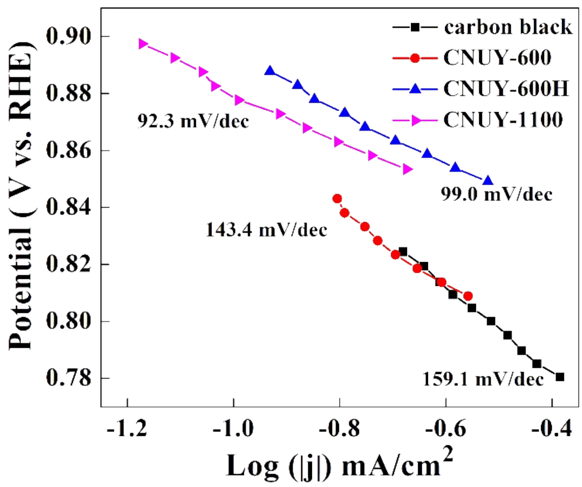

Fig. S16: Tafel plots of the samples used in this work.

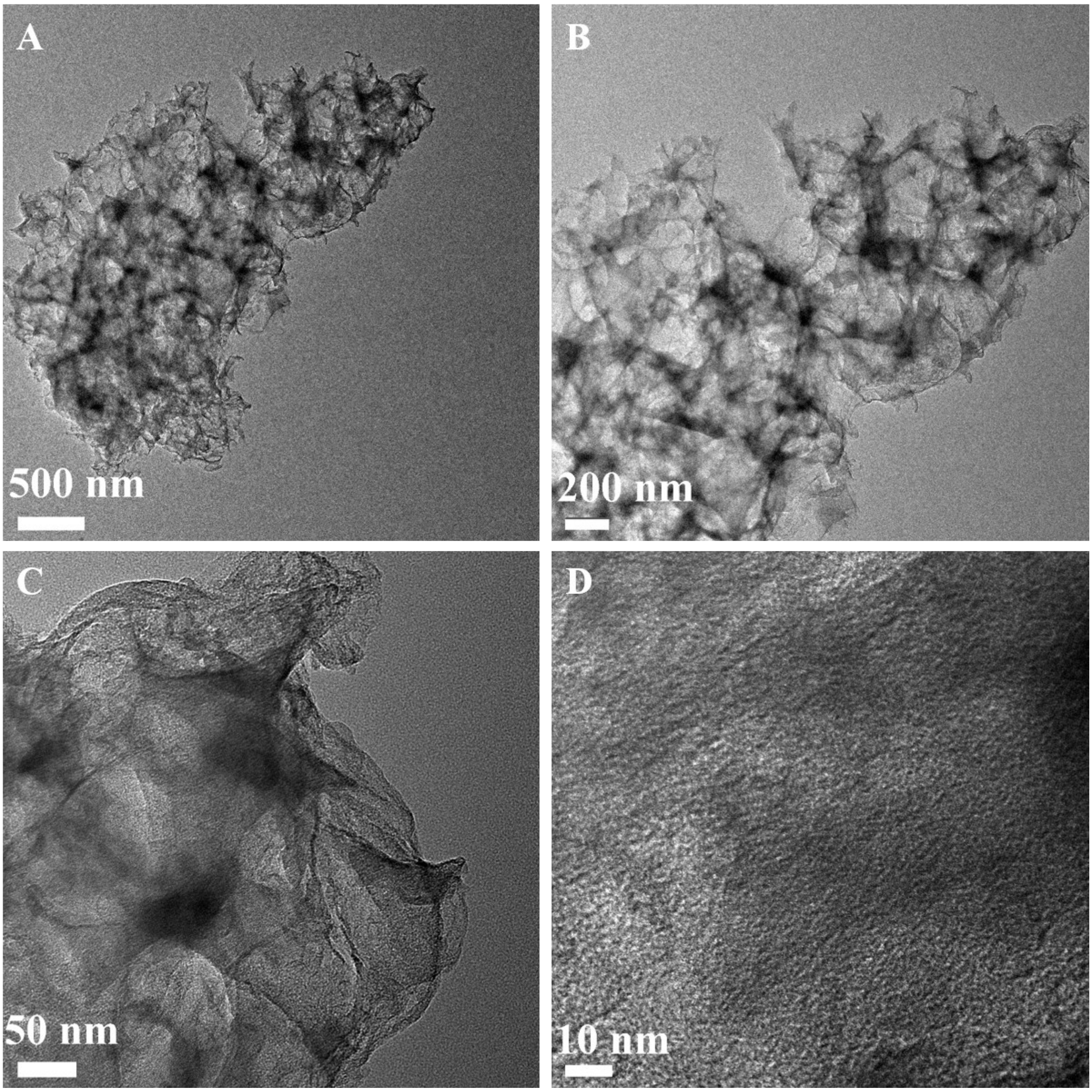

Fig. S17: TEM images of sample CNUY-1100.

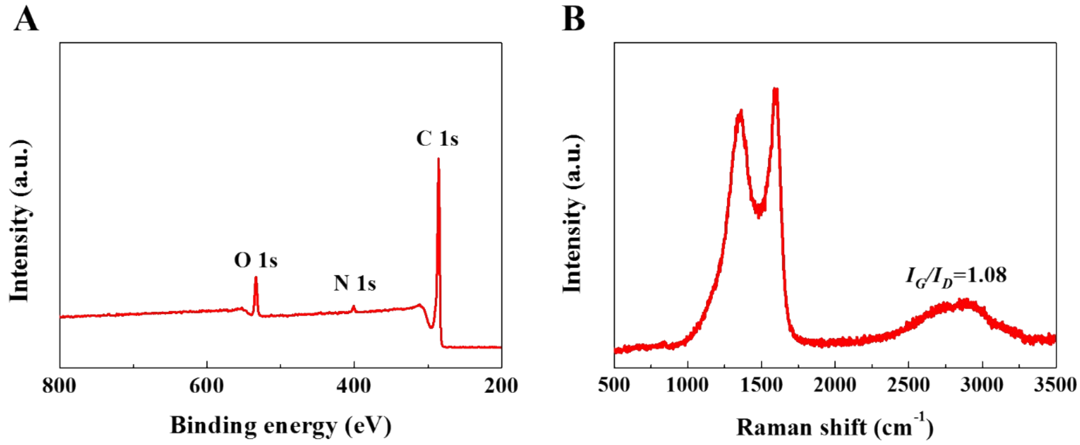

Fig. S18: XPS spectrum (A) and Raman spectra (B) of CNUY-1100

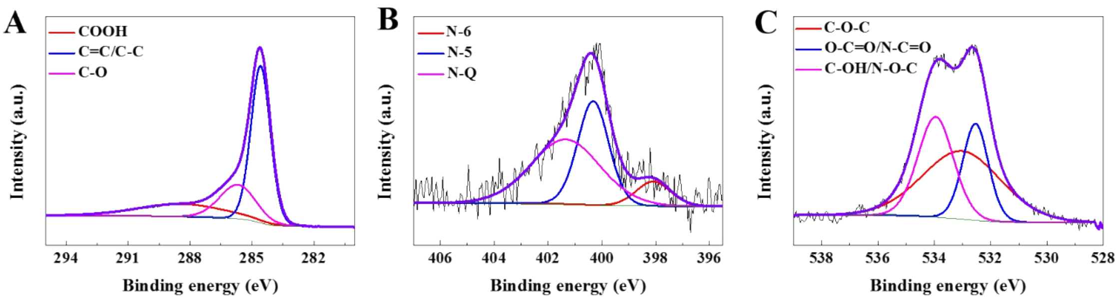

Fig. S19: The deconvoluted C 1s (A), N 1s (B), O 1s (C) spectra of sample CNUY-1100.

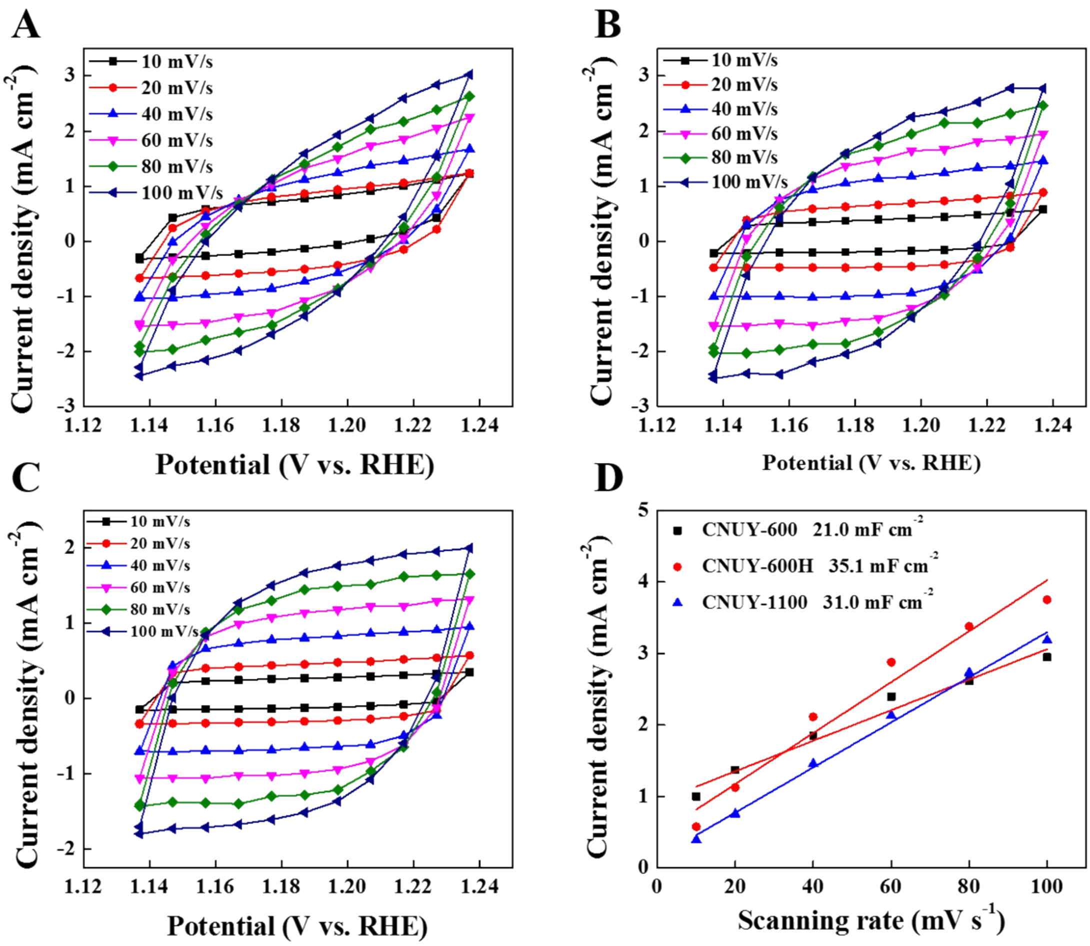

Fig. S20: CV curves of CNUY-600 (A), CNUY-600H (B) and CNUY-1100 (C) catalysts; their capacitive current measured at ~1.2 V vs. RHE plotted as a function of scan rate (D).

Electrochemically active surface area (ECSA) of catalyst plays a crucial role in the reactions. To calculate the ECSA of CNUYs, we conducted CV at different scan rates with a potential window of 1.13~1.23 V vs RHE, where there is no Faradic current. The ECSA was estimated from the as obtained double-layer capacitance (C_{dl}):

$$ECSA = Cdl/Cs \tag{6}$$

C_s is the specific capacitance value for a flat standard with 1 cm^2 of real surface area.

The ECSAs of CNUYs were calculated to compare the active sites, as shown in Fig 6B. ECSA of CNUY-1100 is significantly larger than CNUY-600 but smaller than CNUY-600H. This is because the high temperature (1100°C) destroyed the pore structure to some extent (as shown in the TEM images in Fig. S13), leading to a smaller SSA thus smaller ECSA.

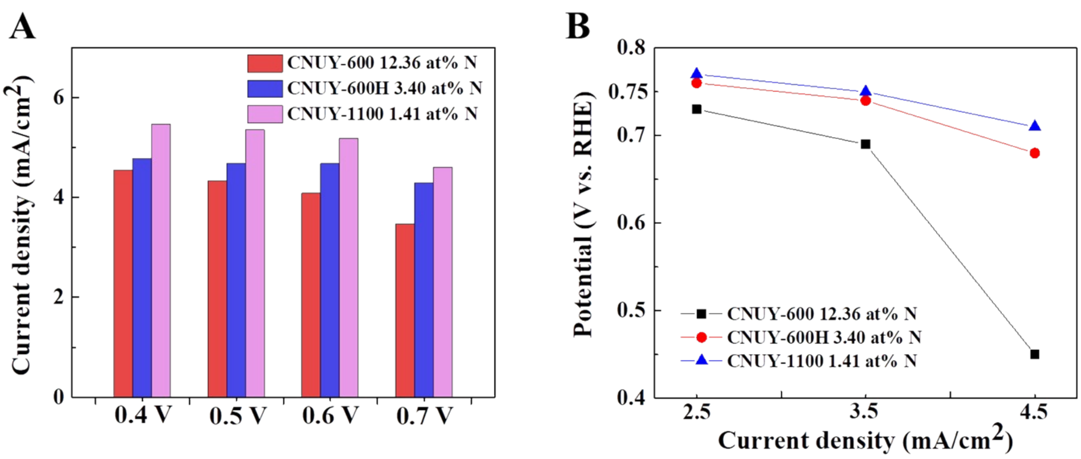

Fig. S21: ORR performance comparison of CNUYs: (A) current densities corresponding to certain potential and (B) potential corresponding to different current densities.

Table. S1 N 1s fitting results of CNUY-600 and CNUY-600H.

Sample	Nitrogen		
	Pyrrolic N	Pyridinic N	Quaternary N
CNUY-600	53.94 %	22.03 %	24.03 %
CNUY-600H	45.87 %	19.07 %	35.05 %

Table. S2 Specific capacitance values (in F/g) of electrodes CNUY-600 and CNUY-600H measured in a three-electrode system with 1 M H_2SO_4 aqueous electrolyte

Current density (A/g)	0.25	0.5	1	2	5	10	20	30	50	80	100
CNUY-600	295	255	244	237	220	200	184	161	134	97	80
CNUY-600H	426	378	346	325	309	277	262	254	231	185	177

Table. S3 Electrochemical performance of electrode CNUY-600 measured in a two-electrode system with 1 M H_2SO_4 as the aqueous electrolyte

Current density (A/g)	0.2	0.5	1	2	5	10	15	20
C_m (F/g)	196	192	187	175	146	123	97	80
Energy density (Wh/Kg)	11.5	11.3	10.9	10.3	8.6	7.2	6.8	4.7
Power density (W/Kg)	162	325	643	1301	3259	6480	11657	13015

Table. S4 Electrochemical performance of electrode CNUY-600H measured in a two-electrode system with 1 M H_2SO_4 as the aqueous electrolyte

Current density (A/g)	0.2	0.5	1	2	5	10	15	20
C_m (F/g)	253	234	228	216	200	185	167	148
Energy density (Wh/Kg)	14.9	13.7	13.4	12.7	11.7	10.9	9.8	8.7
Power density (W/Kg)	131	325	652	1306	3240	6540	9800	13050

Table. S5 Electrochemical performance of electrode CNUY-600H in a symmetric cell with 1M LiCl as the aqueous electrolyte

Current density (A/g)	0.5	1	2	5	10
C_m (F/g)	206	174	156	135	118
Energy density (Wh/Kg)	20.7	17.5	15.7	13.6	11.9
Power density (W/Kg)	426	851	1713	4451	9520

Table. S6 Specific capacitance values of electrode CNUY-600H in a symmetric cell with 2 M KOH as the aqueous electrolyte

Current density (A/g)	0.2	0.5	1	2	5	10	20	30	40	50
C_m (F/g)	176	176	175	168	160	140	128	108	96	80

Table. S7 Areal capacitance values (mF/cm^2) of electrode CNUY-600H of different mass loadings measured in a two-electrode system with 1 M H_2SO_4 as the aqueous electrolyte.

Current density (mA/cm^2)	0.5	1	2	5	10	15	20	30	40	50
1 (mg/cm^2)	243	228	223	210	200	185	162	136	116	74
4 (mg/cm^2)	854	831	800	724	647	600	554	462	370	308
8 (mg/cm^2)	1775	1713	1661	1523	1416	1339	1231	1150	985	923
12 (mg/cm^2)	2518	2465	2338	2246	2000	1846	1723	1569	1354	1128
20 (mg/cm^2)	3988	3877	3662	3246	2779	2308	1908	1477	985	693

Table. S8 Comparison of samples studied in this work.

	CNUY-600		CNUY-600H		CNUY-1100	
	12.36 at% **N**	22.39 at% **O**	3.40 at% **N**	7.43 at% **O**	1.41 at% **N**	6.66 at% **O**
Specific capacitance (F/g, 0.25 A/g)	295		426		93.3	
Specific capacitance (F/g, 100 A/g)	80		177		-	
Onset potential (V vs. RHE)	0.82		0.88		0.90	
Half-wave potential (V vs. RHE)	0.72		0.77		0.77	
Limiting diffusion current (mA/cm^2)	4.59		4.75		5.44	

Table. S9 Comparison of cellulose-derived carbon materials as symmetric SC electrodes

Precursor	Specific capacitance (F/g)	Measurement conditions	Electrolyte	Ref.
Cellulose filter paper	120	1 A/g	2 M KOH	[1]
Bagasse-derived cellulose	142	0.5 A/g	KOH/PVA Gel	[2]
Cellulose acetate	160	0.5 A/g	6 M KOH	[3]
Microcrystal cellulose	194	0.2 A/g	1 M NaCl	[4]
Paper cellulose	200	20 $\mu A/cm^2$	1 M H_2SO_4	[5]
Nanofibrillated cellulose	81	1 mV/s	Solid electrolyte	[6]
Cellulose nanofiber	207	5 mV/s	H_2SO_4/PVA	[7]
Microcrystal cellulose	248	0.1 A/g	1 M H_2SO_4	[8]
Cellulose/MnO_2	306	10 mV/s	1 M Na_2SO4	[9]
Microcrystal cellulose	253	0.2 A/g	1 M H_2SO_4	This work

References

1. W. Luo, B. Wang, C. G. Heron, M. J. Allen, J. Morre, C. S. Maier, W. F. Stickle and X. Ji, *Nano letters*, 2014, **14**, 2225-2229.
2. P. Hao, Z. Zhao, J. Tian, H. Li, Y. Sang, G. Yu, H. Cai, H. Liu, C. Wong and A. Umar, *Nanoscale*, 2014, **6**, 12120-12129.
3. L. Deng, R. J. Young, I. A. Kinloch, A. M. Abdelkader, S. M. Holmes, D. A. De Haro-Del Rio and S. J. Eichhorn, *ACS applied materials & interfaces*, 2013, **5**, 9983-9990.
4. C. Wang, X. Wang, H. Lu, H. Li and X. Zhao, *Carbon*, 2018, **140**, 139-147.
5. L. Hu, J. W. Choi, Y. Yang, S. Jeong, F. La Mantia, L.-F. Cui and Y. Cui, *Proceedings of the National Academy of Sciences*, 2009, **106**, 21490-21494.
6. F. Jiao, J. Edberg, D. Zhao, S. Puzinas, Z. U. Khan, P. Mäkie, A. Naderi, T. Lindström, M. Odén and I. Engquist, *Advanced Sustainable System*, 2018, **2**, 1700121.
7. K. Gao, Z. Shao, J. Li, X. Wang, X. Peng, W. Wang and F. Wang, *Journal of Materials Chemistry A*, 2013, **1**, 63-67.
8. H. Lu, X. Sun, R. R. Gaddam, N. A. Kumar and X. S. Zhao, *Journal of Power Sources*, 2017, **360**, 634-641.
9. L.M. Chen, H.Y. Yu, D.C. Wang, T. Yang, J. Yao, K. C. Tam, *ACS Sustainable Chem. Eng*, 2019, **7**, 11823-11831.